Global deuteron optical model potential for the energy range up to 183 MeV

Haixia An and Chonghai Cai*
Department of Physics, Nankai University, Tianjin 300071, China
(Received 27 January 2006; published 8 May 2006)

Based on the existing experimental data of elastic scattering angular distributions and nonelastic cross sections (i.e., total reaction cross sections) for incident deuteron, by using the modified code APMN, we obtain a new optimal set of global deuteron optical potential parameters, which can fit (or reproduce) the experimental data very well for almost all target nuclei ranging from ^{12}C to ^{238}U in the energy region below 183 MeV.

DOI: 10.1103/PhysRevC.73.054605 PACS number(s): 24.10.Ht, 25.40−h, 25.45.De

I. INTRODUCTION

The optical model is the basis and starting point for all nuclear model calculations. There are many successful local and global optical model parameters for reactions induced by neutrons and protons, and it is of interest to probe into the optical model potential for reactions induced by incident deuterons, the deuteron being a weakly bound composite particle. Previous studies focused on searching for either the best-fit parameters for individual nuclei or for global fit parameters that then depend on energy and mass number.

There are mainly three important sets of global optical model potentials available for the deuteron as a projectile. The first one was established by C. M. Perey and F. G. Perey [1], which was in popular use for nuclear model calculations during earlier times (usually deuteron was one of the outgoing particles). The second one was developed by W. W. Daehnick *et al*. [2], which covered a target mass range of $27 \leqslant A \leqslant 238$ and an energy range from 11.8 to 90 MeV. The third set was supplied by J. Bojowald *et al*. [3], which covered a target mass range of $12 \leqslant A \leqslant 208$ and the energy range from 52 to 85 MeV. A. C. Betker *et al*. [4] used the optical potentials of Daehnick *et al*. and Bojowald *et al*. to analyze their 110- and 120-MeV data for ^{12}C, ^{58}Ni, and ^{208}Pb, in 1993. Bäumer *et al*. [5] also applied the above two potentials to their 170-MeV data for ^{12}C, ^{24}Mg, ^{58}Ni, in 2001; as did A. Korff *et al*. [6], in 2004, to their 171-MeV data for ^{6}Li, ^{16}O, ^{32}S, ^{50,51}V, and ^{70,72}Ge and their 183-MeV data for ^{90}Zr and ^{116}Sn. They all found that, for incident deuteron energies higher than 100 MeV, the elastic scattering angular distributions calculated with the optical potentials of Daehnick *et al*. and Bojowald *et al*. were in worse agreement with their experimental data, especially for large angles. To better fit their experimental data, they started from the optical potentials of Daehnick *et al*. and Bojowald *et al*. and found two sets of local fit parameters (each for a single target nucleus and single energy) and called them *D* fit and *B* fit, respectively.

Up to now, there is no set of global parameters that can describe these new experimental data above 100 MeV. Therefore, it is necessary to find a new optimal set of global optical potential parameters. In this work we plan to extend the highest energy to 183 MeV. However, polarized data are not included.

All optical potentials of Daehnick *et al*. and Bojowald *et al*., and those used here have the same general form [see Eqs. (1) and (2)]. The differences are the different dependence on bombarding energy and target mass number of the depth of the potential well and geometric parameters. The surface (W_s) and volume (W_v) absorption of the imaginary potential of Daehnick *et al*., were functions of a constant plus linear energy term multiplied by a factor $(1 - e^{\beta})$ and e^{β} $[\beta = -(E/100)^2]$, respectively. The constant, the linear energy term, and the $A^{1/3}$ terms were included in W_s of Bojowald *et al*. and only the constant and the linear energy term were included in W_v, which was zero for incident energies less than 45 MeV. Consequently, only surface absorption was effective in the energy region 0–45 MeV for the potential of Bojowald *et al*. For the spin-orbit potential, the real part V_{so} of Daehnick *et al*. was a function of the bombarding energy and that of Bojowald *et al*. was a constant. The imaginary part W_{so} of the *L*-*S* coupling potential was not included in the potentials of Daehnick *et al*. and Bojowald *et al*. The diffusiveness parameter a_r of the real part in the potential of Daehnick *et al*. was a function of incident energy and that of Bojowald *et al*. was a function of $A^{1/3}$. For the diffusiveness parameter a_I of the imaginary part of the potential, a shell effect was considered in Daehnick *et al*. ($a_I = 0.53 + 0.07\,A^{1/3} - 0.04\,\Sigma_i e^{-\mu_i}$, $\mu_i = [(M_i - N_i)/2]^2$, M_i = magic numbers), and it was a function of $A^{1/3}$ for Bojowald *et al*.; a_I was the same for the surface and volume imaginary potential in both the Daehnick and Bojowald potentials. For Daehnick *et al*., r_r, r_I, r_{so}, r_C, and a_{so} were all constants, and for Bojowald *et al*., r_r, r_I, and r_C were constants and the r_{so} and a_{so} were a function of $A^{1/3}$ and equal to each other.

APMN [7] is a code that searches automatically for a set of optimal optical potential parameters with the smallest χ^2 for $E \leqslant 300$ MeV by means of an improved steepest descent algorithm [8]. The optical potentials in APMN are of standard BG (Becchetti and Greenlees [9]) form, i.e., a Woods-Saxon form for the real part and the imaginary part corresponding to volume absorption; a derivative Woods-Saxon form for the imaginary part corresponding to surface absorption; and a Thomas form for the spin-orbital potential. The Coulomb potential V_C is also included. Based on existing deuteron experimental data of elastic scattering angular distributions and nonelastic cross sections, and using the modified code

*Electronic address: haicai@nankai.edu.cn

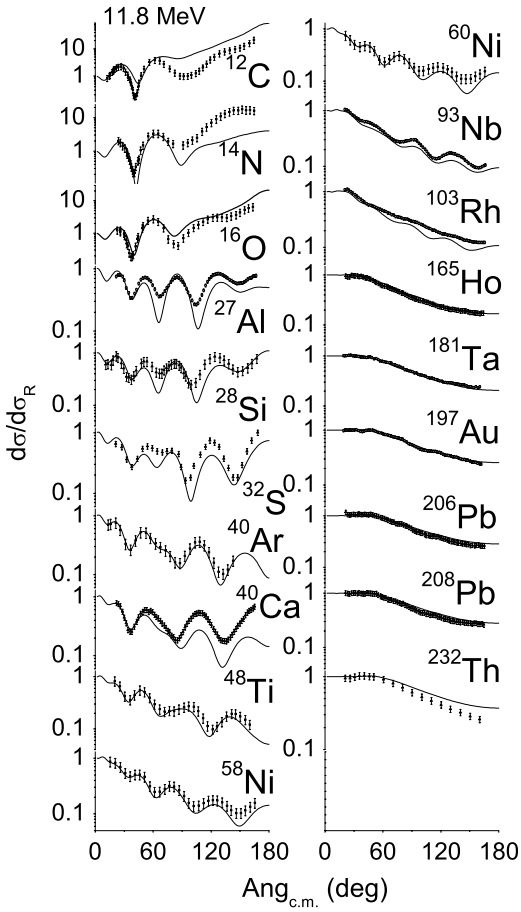

FIG. 1. Comparison of 11.8-MeV elastic scattering data of Refs. [11–13] with the values from our global potential. The data of ^{40}Ca, ^{60}Ni, ^{165}Ho, and ^{206}Pb have not been included in the global parameter search.

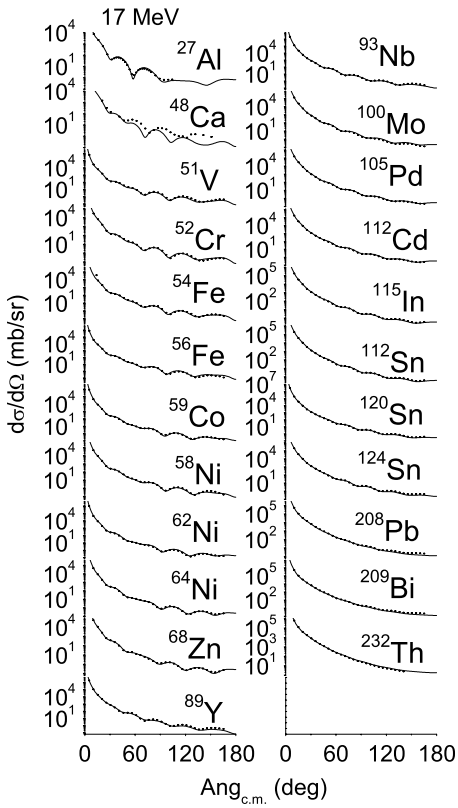

FIG. 2. Comparison of 17-MeV elastic scattering data of Ref. [14] with the values from our global potential. The data of ^{48}Ca, ^{59}Co, ^{62}Ni, ^{64}Ni, ^{105}Pd, ^{112}Cd, ^{115}In, ^{112}Sn, ^{124}Sn, and ^{209}Bi have not been included in the global parameter search.

APMN and the potential by C. M. Perey and F. G. Perey as a starting point, we plan to search for a new set of parameters for a global deuteron potential in a wider energy range and for more target nuclei than other global deuteron potentials.

This article is arranged as follows. Section II describes our optical model and global optical potential parameters, and Sec. III presents the database for searching for global optical potential parameters. Section IV is a comparison of our work with a previous work [3], Sec. V describes the results and discussion, and Sec. VI provides a summary.

II. OPTICAL MODEL AND GLOBAL OPTICAL POTENTIAL PARAMETERS

In APMN, all radius and diffusiveness parameters are constant, they do not vary with mass number of the target nucleus. In this work, according to the global optical model parameters (OMP) of Varner *et al.* [10], the radius parameters are taken in the form of $r_i = r_{i0} + r_{i1}\,A^{-1/3}$. Following Bojowald *et al.* [3], the diffusiveness parameters are taken in the form of $a_i = a_{i0} + a_{i1}\,A^{1/3}$. We also made some other small changes in APMN to allow it to contain the parameters in the form given in Ref. [3]. The code APMN as modified by us contains 33 adjustable parameters.

The optical model potential in the modified APMN code is given as follows:

$$V(r) = -V\,f_r(r) - i\,W_v\,f_v(r) + i\,4\,a_s W_s\,\frac{df_s(r)}{dr} + \lambda_\pi^2\,\frac{V_{so}+W_{so}}{r}\,\frac{df_{so}(r)}{dr}\,\vec{\sigma}\cdot\vec{l} + V_C(r), \quad (1)$$

where

$$f_i(r) = \{1+\exp[(r - r_i\,A^{1/3})/a_i]\}^{-1} \quad \text{with} \quad i = r, v, s, \text{so}, \quad (2)$$

$$V = V_0 + V_1\,E_d + V_2\,E_d^2 + V_3\,(N-Z)/A + V_4\,Z/A^{1/3}, \quad (3)$$

$$W_s = W_{s0} + W_{s1}\,E_d + W_{s2}\,(N-Z)/A + W_{s3}\,A^{1/3}, \quad (4)$$

$$W_v = \begin{cases} W_{v0} + W_{v1}\,E_d + W_{v2}\,E_d^2 & : \quad E_d \leqslant E_{\text{bd}} \\ W_{v0h} + W_{v1h}\,E_d + W_{v2h}E_d^2 & : \quad E_d > E_{\text{bd}} \end{cases} \quad (5)$$

$$R_i = r_i\,A^{1/3} \quad \text{with} \quad i = r, v, s, \text{so}, C, \quad (6)$$

$$r_i = r_{i0} + r_{i1}\,A^{-1/3} \quad \text{with} \quad i = r, v, s, \text{so}, \quad (7)$$

$$a_i = a_{i0} + a_{i1}\,A^{1/3} \quad \text{with} \quad i = r, v, s, \text{so}, \quad (8)$$

where E_d is the incident deuteron energy in the laboratory frame and Z, N, and A are the number of protons, neutrons,

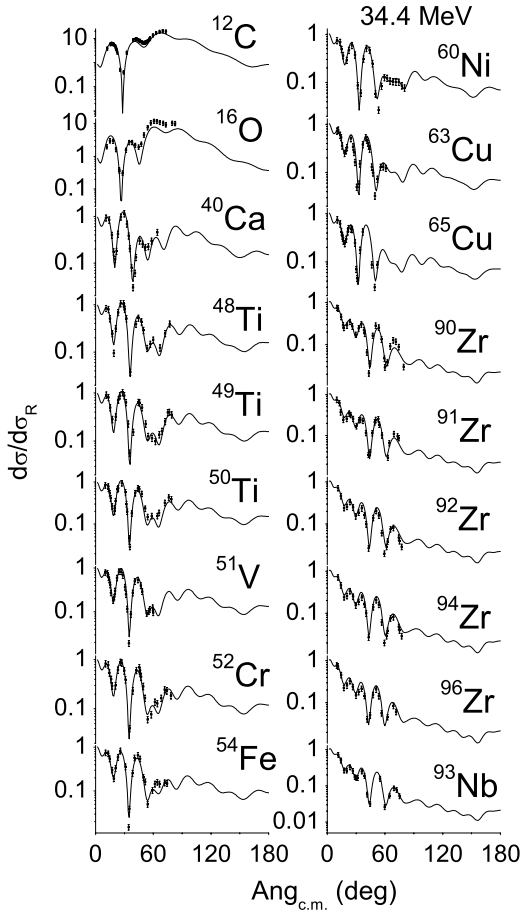

FIG. 3. Comparison of the 34.4-MeV elastic scattering data of Ref. [15] with the values from our global potential. The data of ^{49}Ti, ^{50}Ti, ^{60}Ni, ^{91}Zr, ^{92}Zr, ^{94}Zr, and ^{96}Zr have not been included in the global parameter search.

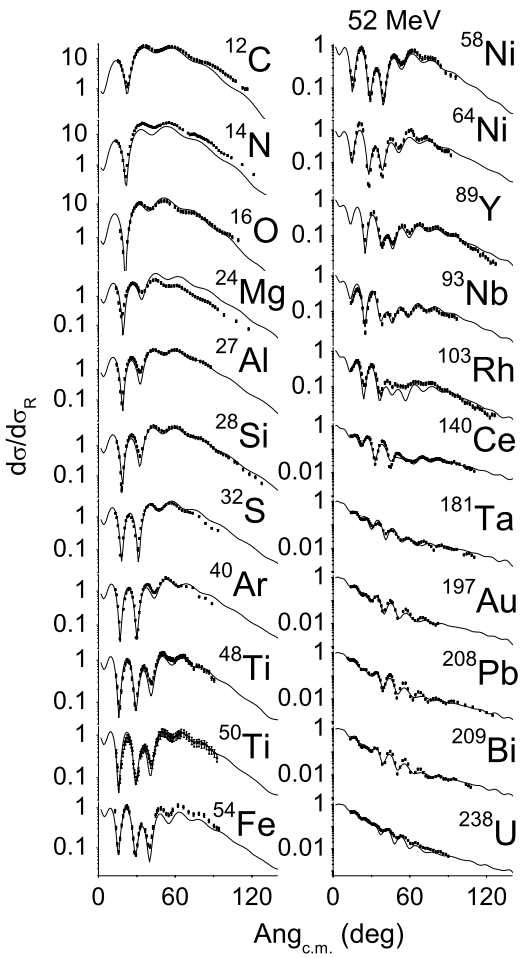

FIG. 4. Comparison of the 52-MeV elastic scattering data of Ref. [16] with the values from our global potential. The data of ^{50}Ti and ^{64}Ni have not been included in the global parameter search.

and the nucleons of the target nucleus, respectively. $E_{\rm bd}$ is the energy boundary in W_v. V is the real part potential, W_s and W_v are the surface and volume absorption of the imaginary part potential, respectively, and $V_C(r)$ is the Coulomb potential and is taken as a potential of uniformly charged sphere with radius R_C.

Considering that the isospin of deuteron is zero, we let $V_3 = 0$, $W_{s2} = 0$. Through a real search, we find that W_{v2}, W_{v2h}, W_{s3}, and $W_{\rm so}$ are almost zero, the difference of W_{v1} and W_{v1h} is very small, and $V_{\rm so}$ is small, so we do not need give W_v in the lower and higher energy regions, respectively, and can take $W_{v2} = 0$, $W_{s3} = 0$, $W_{\rm so} = 0$, $r_{\rm so1} = a_{\rm so1} = 0$ to reduce the number of parameters. Finally, there are only 24 parameters in our optimal set of global deuteron optical potential parameters; they can be read as:

$$V = 91.85 - 0.249\,E_d + 0.000116\,E_d^2 + 0.642\,Z/A^{1/3}, \tag{9}$$

$$W_s = 10.83 - 0.0306\,E_d, \quad W_v = 1.104 + 0.0622E_d, \tag{10}$$

$$V_{\rm so} = 3.557,$$

$$a_r = 0.719 + 0.0126\,A^{1/3}, \quad a_s = 0.531 + 0.062\,A^{1/3}, \tag{11}$$

$$a_v = 0.855 - 0.100\,A^{1/3},$$

$$r_r = 1.152 - 0.00776\,A^{-1/3}, \quad r_s = 1.334 + 0.152\,A^{-1/3}, \tag{12}$$

$$r_v = 1.305 + 0.0997\,A^{-1/3},$$

$$a_{\rm so} = 1.011, \quad r_{\rm so} = 0.972, \quad r_C = 1.303. \tag{13}$$

III. THE DATABASE FOR THE GLOBAL PARAMETER SEARCH

All experimental data used in this work are taken from the EXFOR, which benefits the search, because the references concerning our experiment usually give only figures rather than data. All these experimental data are given in the center-of-mass (c.m.) system, so all our calculation values are given in the c.m. system, too. Our theoretical treatment is always in the nonrelativistic frame; no consideration is given to the relativistic kinetics corrections because they are usually very small (below 300 MeV). For example, for an incoming deuteron with a kinetic energy of 300 MeV in the laboratory system, the relativistic correction for the relative kinetic energy

TABLE I. The database for the global parameter search.

Nucleus	Energy (MeV)	Refs.	Nucleus	Energy (MeV)	Refs.
^{12}C	11.8–170	[4,5,13,15,16,18,21,23,33]	^{68}Zn	17.0, 80	[14,18]
^{14}N	11.8, 52,	[13,16]	^{70}Ge	171	[6]
^{16}O	11.8–171	[6,13,15–17,33]	^{72}Ge	171	[6]
^{24}Mg	52–90	[5,16,17,28]	^{89}Y	17.0–85.0	[3,14,16,18]
^{27}Al	11.8–85	[3,11,14,16,18,24]	^{90}Zr	34.4–183	[6,15,17,38]
^{28}Si	11.8–97.4	[13,16,17,33]	^{93}Nb	11.8–52	[11,14–16]
^{32}S	11.8–171	[6,12,16,17]	^{100}Mo	17	[14]
^{40}Ar	11.8–56.0	[13,16,17]	^{103}Rh	11.8,52.0	[11,16]
^{40}Ca	34.4–140	[15,17,21,33]	^{116}Sn	37.9–183	[6,33]
^{48}Ti	11.8–52.0	[13,15,16,35]	^{120}Sn	17.0–97.4	[3,14,33]
^{50}V	171	[6]	^{140}Ce	52.0	[16]
^{51}V	13.6–171	[6,14,15,35]	^{181}Ta	11.8,52	[11,16]
^{52}Cr	13.6–34.4	[14,15,35]	^{197}Au	11.8,52	[11,16]
^{54}Fe	17.0–56.0	[14–17]	^{208}Pb	11.8–140	[3,4,12,14,16–18,21,33]
^{56}Fe	11.8–56.0	[14,36,39]	^{209}Bi	52.0	[16]
^{58}Ni	11.8–170	[4,5,13,14,16–18,25,33]	^{232}Th	11.8–70	[12,14,38]
^{63}Cu	11.93–34.4	[15,37]	^{238}U	52.0	[16]
^{65}Cu	11.0–34.4	[15,37]			

in the c.m. system is 0.26% for ^{58}Ni, 0.97% for ^{12}C; at most 1.47% even for ^{6}Li.

As few experimental data exist for incident energies higher than 183 MeV, these data, such as the 200-MeV data of ^{12}C and ^{58}Ni, and the 270-MeV data of ^{12}C and ^{40}Ca, are not used for the global parameter search and are utilized for testing the predictive power of the obtained global parameters. We find that it is reasonable to use the derived parameters. And it is also acceptable to not use data that are lower than 183 MeV when searching for the global parameters. The light nucleus ^{6}Li is not included in our mass range for the global parameter search, but a reasonable result is obtained when using the present parameters of 171 MeV. There are 35 nuclei, 122 sets of angular distributions of elastic scattering, and 11 sets nonelastic cross sections experimental data that are included in searching for the optimal global parameters. The database is shown in Table I.

IV. COMPARISON WITH THE GLOBAL POTENTIAL OF BOJOWALD *ET AL.*

The form of global potential parameters of Bojowald *et al*. is contained in modified APMN code, so we can directly use it to calculate the χ^2 of the potential of Bojowald *et al*. and of our global potential. The global potential parameters of Daehnick *et al*. are not contained in the modified APMN code. Although we rewrite another code specially used for the potential of Daehnick *et al*., we cannot reproduce their angular distribution curves and get a much larger χ^2 [2]. We checked the code several times but still did not find the reason. So we compare the χ^2 of our global potential parameters only with those of the global potential parameters of Bojowald *et al*.

The χ^2 represents the deviation of the calculated values from the experimental data, and it is defined as follows:

$$\chi^2 = \frac{1}{NN}\sum_{n=1}^{NN}\chi_n^2 \tag{14}$$

$$\chi_n^2 = \frac{\frac{W_{n,\mathrm{non}}}{N_{n,\mathrm{non}}}\sum_{i=1}^{N_{n,\mathrm{non}}}\left(\frac{\sigma_{\mathrm{non,i}}^{th}-\sigma_{\mathrm{non,i}}^{\mathrm{exp}}}{\Delta\sigma_{\mathrm{non,i}}^{\mathrm{exp}}}\right)^2 + \frac{W_{n,\mathrm{el}}}{N_{n,\mathrm{el}}}\sum_{i=1}^{N_{n,\mathrm{el}}}\frac{1}{N_{n,i}}\sum_{j=1}^{N_{n,i}}\left(\frac{\sigma_{\mathrm{el}}^{\mathrm{th}}(i,j)-\sigma_{\mathrm{el}}^{\mathrm{exp}}(i,j)}{\Delta\sigma_{\mathrm{el}}^{\mathrm{exp}}(i,j)}\right)^2}{W_{n,\mathrm{non}}+W_{n,\mathrm{el}}}. \tag{15}$$

χ_n^2 is for a single nucleus, and χ^2 is for multiple nuclei in the database for the global parameter search. Letter n represents the nucleus sequence number, NN denotes the numbers of nuclei included in the global parameter search; here $NN = 35$. $W_{n,\mathrm{non}}$ and $N_{n,\mathrm{non}}$ are the weight and the energy points number of nonelastic cross sections, as are the $W_{n,\mathrm{el}}$ and $N_{n,\mathrm{el}}$ of angular distribution of elastic scattering; $N_{n,i}$ is the number of angles for n-th nucleus and i-th incidence energy. We believe that experimental data of all nuclei are reliable; equal weight is applied with $W_{n,\mathrm{non}} = 0.1$ and $W_{n,\mathrm{el}} = 2.0$. Obviously, there are much more angular distributions of elastic scattering experimental data than nonelastic cross sections, and it seems easier to fit the experimental data of nonelastic cross section, so a much larger $W_{n,\mathrm{el}}$ than $W_{n,\mathrm{non}}$ is reasonable. Table II shows the χ_n^2 of each nucleus for two sets of global potential parameters, and those nuclei not included in the

TABLE II. χ_n^2 of each nuclei for two different potentials.

Nucleus	This work	Bojowald	Nucleus	This work	Bojowald	Nucleus	This work	Bojowald
^{6}Li	25.25	177.31	^{56}Fe	26.72	49.30	^{92}Mo	0.39	2.00
^{12}C	14.33	402.37	^{59}Co	30.92	352.21	^{100}Mo	23.66	16.99
^{14}N	195.88	189.61	^{58}Ni	13.24	2487.7	^{103}Rh	29.62	62.44
^{16}O	24.20	61.12	^{60}Ni	8.48	28.19	^{105}Pd	10.58	99.41
^{24}Mg	17.55	74.18	^{62}Ni	9.45	47.28	^{112}Cd	13.19	92.55
^{27}Al	176.01	1298.05	^{64}Ni	11.54	105.54	^{112}Sn	34.73	170.16
^{28}Si	6.45	21.21	^{63}Cu	7.48	8.13	^{116}Sn	4.78	85.41
^{32}S	46.63	99.21	^{65}Cu	5.25	8.44	^{120}Sn	8.55	17.83
^{40}Ar	10.25	42.2	^{68}Zn	11.52	45.99	^{124}Sn	16.82	61.02
^{40}Ca	3.59	66.94	^{70}Ge	6.47	117.85	^{140}Ce	54.40	556.23
^{48}Ca	123.58	178.41	^{72}Ge	2.21	300.45	^{165}Ho	0.52	0.94
^{48}Ti	2.87	8.09	^{89}Y	40.59	113.14	^{181}Ta	18.92	116.67
^{49}Ti	3.58	19.50	^{90}Zr	4.03	21.06	^{197}Au	2.20	11.27
^{50}Ti	1.67	5.90	^{91}Zr	2.15	8.42	^{206}Pb	1.02	0.16
^{50}V	2.09	84.87	^{92}Zr	6.48	11.69	^{208}Pb	17.42	43.80
^{51}V	8.68	74.90	^{94}Zr	3.49	12.75	^{209}Bi	3.84	21.20
^{52}Cr	30.56	218.70	^{96}Zr	13.39	62.60	^{232}Th	35.74	14.11
^{54}Fe	24.16	135.69	^{93}Nb	11.51	50.81	^{238}U	5.47	6.11

global parameter search are also listed. The χ^2 of the 35 nuclei are 25.53 and 170.61 for this work and Bojowald *et al*., respectively. From Table II we can clearly see that the χ_n^2 of our global parameters are obviously smaller than those of the global parameters of Bojowald *et al*. for most target nuclei except several nuclei, such as ^{54}Fe, ^{100}Mo, ^{206}Pb, and ^{232}Th. For our global parameters, χ_n^2 is greater than 100 only for ^{14}N, ^{27}Al, and ^{48}Ca and smaller than 55 for all other nuclei.

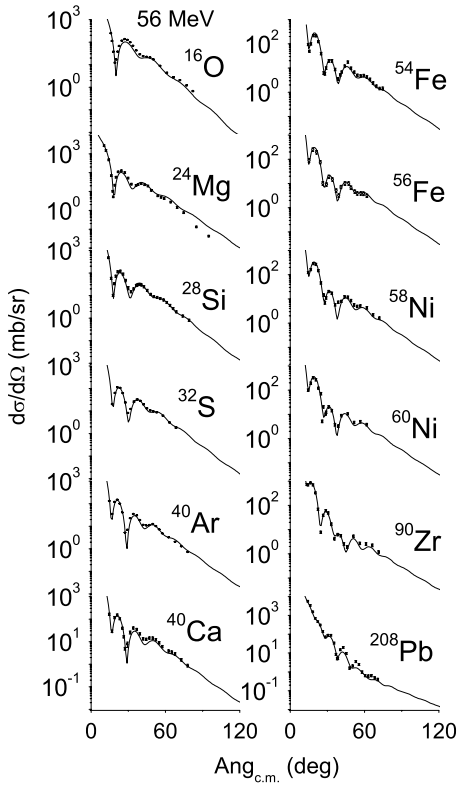

FIG. 5. Comparison of the 56-MeV elastic scattering data with the values from our global potential. The data of ^{56}Fe are from Ref. [39], and the remainder are from Ref. [17]. The data of ^{60}Ni have not been included in the global parameter search.

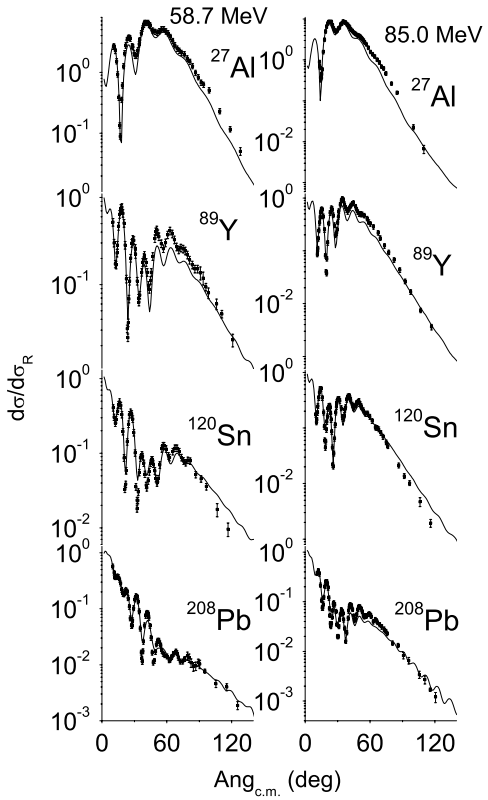

FIG. 6. Comparison of the 58.7- and 85-MeV elastic scattering data of Ref. [3] with the values from our global potential.

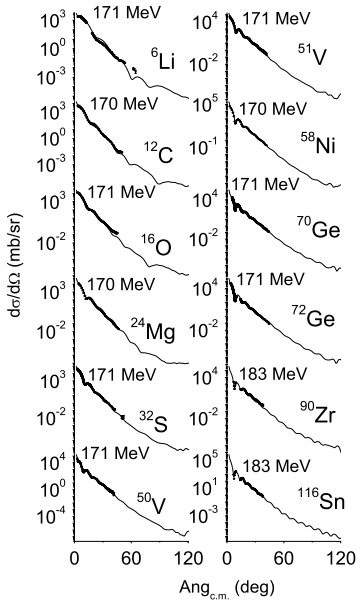

FIG. 7. Comparison of elastic scattering data with the values from our global potential. The data at 170 MeV are from Ref. [5], and those at 171 and 183 MeV are from Ref. [6]. The data of ^{6}Li have not been included in the global parameter search.

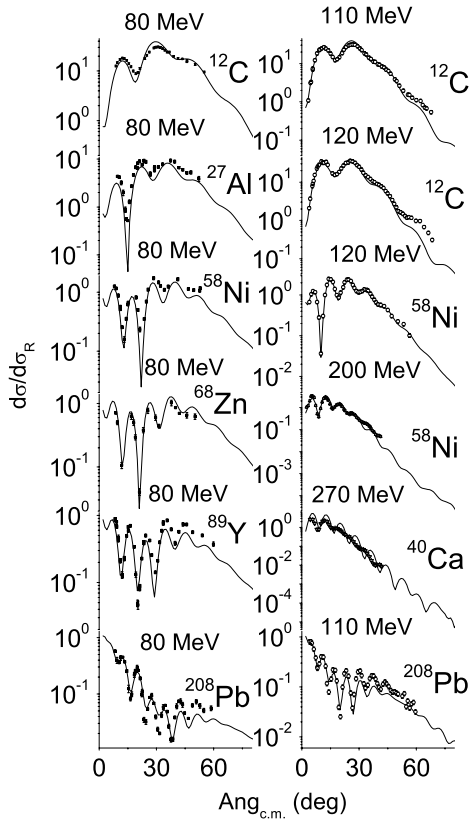

FIG. 8. Comparison of elastic scattering data with the values from our global potential. The data at 80 MeV are from Ref. [18], data at 110 and 120 MeV are from Ref. [4], data at 200 MeV are from Ref. [19], and those at 270 MeV are from Ref. [20]. The data of ^{58}Ni at 200 MeV and those of ^{40}Ca at 270 MeV have not been included in the global parameter search.

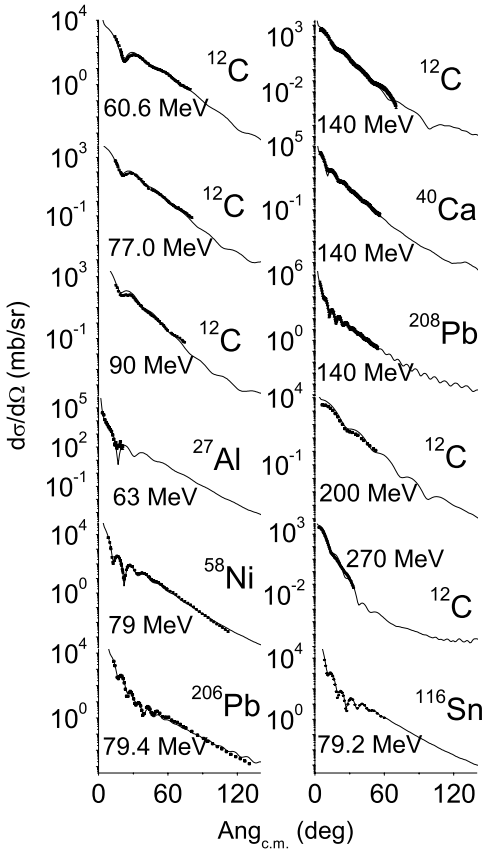

FIG. 9. Comparison of elastic scattering data with the values from our global potential. The data at 140 MeV are from Ref. [21]; data at 270 MeV are from Ref. [22]; data at 60.6, 77, and 90 MeV of ^{12}C are from Ref. [23]; data at 200 MeV of ^{12}C are from Ref. [34]; data at 63 MeV of ^{27}Al are from Ref. [24]; data at 79 MeV of ^{58}Ni are from Ref. [25]; data at 79.4 MeV of ^{206}Pb are from Ref. [26]; and those at 79.2 MeV of ^{116}Sn are from Ref. [27]. The data of ^{12}C at 200 and 270 MeV, ^{116}Sn at 79.2 MeV, and ^{206}Pb at 79.4 MeV have not been included in the global parameter search.

This shows that our optimal set of deuteron global optical potential parameters is of good universality.

V. RESULTS AND DISCUSSION

The theoretical angular distributions of elastic scattering calculated from our global potential parameters and their experimental data are plotted in Figs. 1–11, and the nonelastic cross sections are shown in Fig. 12.

The angular distributions at 11.8 MeV are given in Fig. 1, from which we can see that the theoretical angular distributions are worse in comparison with experimental data for lighter targets, the same as in many preceding studies, such as Daehnick *et al.* [2]. In APMN, the compound nucleus elastic scattering is calculated with Hauser-Feshbach statistic theory with width fluctuation correction (WHF), which is not completely suitable for light target nuclei, such as ^{12}C and ^{14}N; this may be the reason that our theoretical angular distributions are worse at 11.8 MeV for ^{12}C and ^{14}N. As for ^{27}Al, ^{28}Si, ^{32}S, ^{93}Nb, ^{103}Rh, and ^{232}Th, the reasons the theoretical values did

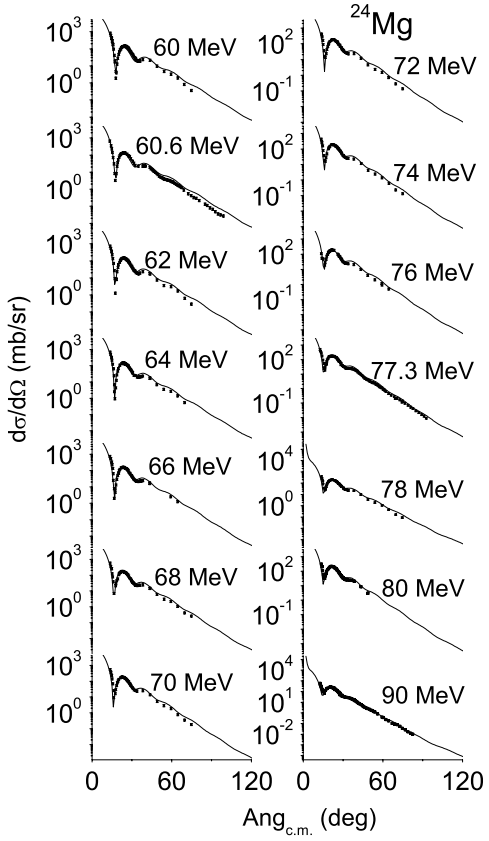

FIG. 10. Comparison of elastic scattering data of Ref. [28] with the values from our global potential of ^{24}Mg.

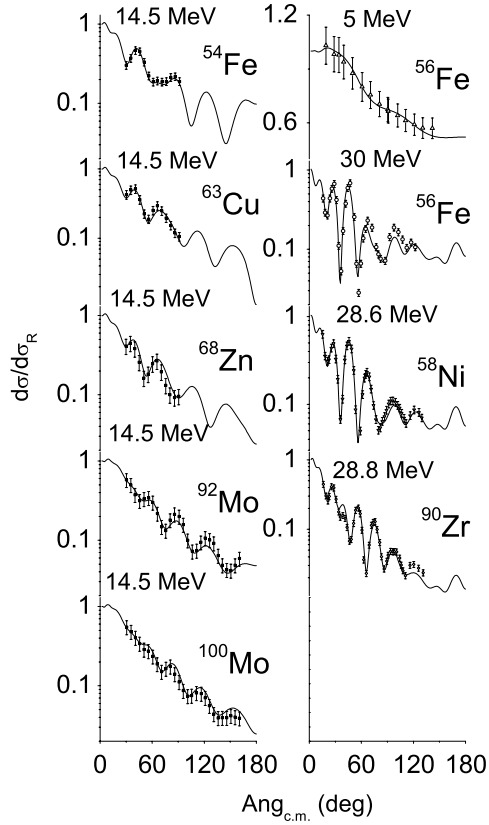

FIG. 11. Comparison of elastic scattering data with the values from our global potential. The data at 14.5 MeV are from Ref. [29], data at 5 MeV are from Ref. [30], data at 30 and 28.8 MeV are from Ref. [31], data at 28.6 MeV are from Ref. [32]. All of the experimental data plotted in this figure have not been included in the global parameter search.

not fit the experimental data are not yet very clear; this may be because of experimental error, may theoretical error, or perhaps both. It should be noted that for the angular distributions of ^{40}Ca at 11.8 MeV (Fig. 1) and that of ^{48}Ca at 17 MeV (Fig. 2), J. D. Childs *et al*. [14] pointed out that the ^{48}Ca data had the largest systematic error, and they could not believe that experimental errors are responsible for this unexpected disagreement. Actually, other studies of elastic scattering of other projectiles from Ca isotopes also have show unexpected behavior [9].

All theoretical angular distributions at 17 MeV shown in Fig. 2 are in very good agreement with experimental data except for ^{48}Ca. From Fig. 3 and Fig. 5 we can see that at 34.4 and 56 MeV, all calculated values are in rather good accordance with experimental data except for ^{16}O at 34.4 MeV. The angular distributions at 52 MeV are plotted in Fig. 4, which shows that the calculated values of ^{24}Mg are worse for angles larger than 45°, the calculated values of seven other nuclei are not very good, and those of the rest of the nuclei are good in comparison with experimental data. Figure 6 gives the angular distributions at 58.7 and 85 MeV; the values of ^{89}Y for angles between 50° and 80° and the values of ^{27}Al and ^{120}Sn in large angles are not in very good agreement with experimental data, whereas those of other nuclei in rather good agreement.

All theoretical angular distributions at 170, 171, and 183 MeV shown in Fig. 7 are consistent with experimental data. We point out that our angular distributions of ^{12}C, ^{24}Mg, and ^{58}Ni at 170 MeV are in good agreement with experimental data as the B-fit of Bäumer *et al*. [5]; our angular distributions of ^{16}O, ^{32}S, ^{50,51}V, and ^{70,72}Ge at 171 MeV and the 183-MeV data of ^{90}Zr and ^{116}Sn are also in good agreement with the experimental data as the B-fit of Korff *et al*. [6]. Our theoretical values are a little worse than the B-fit of Korff *et al*. only for the very light nucleus $7Li$, but much better than the values calculated with the global potentials of Bojowald *et al*. [3] and Daehnick *et al*. [2].

The angular distributions at 80, 110, 120, and 270 MeV are given in Fig. 8, from which we can see that the calculated values are in rather good agreement with experimental data except for ^{12}C at large degrees and ^{40}Ca at 270 MeV, with slightly worse values.

All theoretical angular distributions shown in Figs. 9 and 11 are in rather good agreement with experimental data. The angular distributions of ^{24}Mg at 60–90 MeV are plotted in Fig. 10, and all calculated values are in agreement with experimental data except for large angles at 60.6 MeV with a little larger deviation.

From Figs. 1–11 we can see that the angular distributions of those nuclei (^{6}Li, ^{48}Ca, ^{49,50}Ti, ^{59}Co, ^{60,62,64}Ni, ^{91,92,94,96}Zr, ^{92}Mo, ^{105}Pd, ^{112}Cd, ^{115}In, ^{112,124}Sn) not included in the search for the optimal global parameters are also in rather good

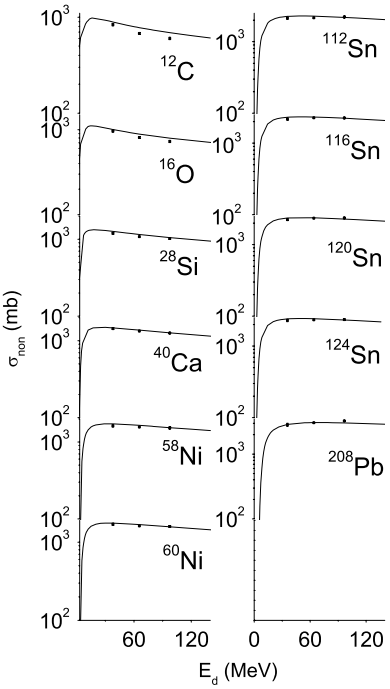

FIG. 12. Comparison of nonelastic scattering data of Ref. [33] with the values from our global potential. The data of ^{112}Sn and ^{124}Sn have not been included in the global parameter search.

agreement with experimental data generally. This means that we found an optimal set of global parameters.

The calculated nonelastic cross sections are plotted in Fig. 12, which are all in good agreement with experimental data.

VI. SUMMARY

Based on the existing experimental data of nonelastic cross sections and elastic scattering angular distributions, we obtained an optimal set of deuteron global optical potential parameters with the modified code APMN, that are available for nuclear model calculations up to about 200 MeV and for almost all nuclei ranging from ^{12}C to ^{238}U. Up to now, there are no sets of global optical potential parameters for neutrons, protons, deuterons, or other light particles as projectiles which that are able to fit experimental data of nonelastic cross sections and elastic scattering angular distributions so well and in such a wide energy range. The shortcoming of this work is that polarized data are not included in the global parameter search. However, in most realistic applications, such as nuclear model calculations, especially in common nuclear data calculations, polarization is usually not considered, so our sets of deuteron global optical potential parameters are very useful. They can be used directly for many nuclei for which experimental data exist as well as for those nuclei for which experimental data are incomplete. For some other nuclei, if this set of parameters cannot fit the experimental data very well, it can be taken as a starting point in further searches for a local best parameter set for a particular target nucleus.

[1] C. M. Perey, and F. G. Perey, At. Data Nucl. Data Tables **13**, 293 (1974); **17**, 1 (1974).
[2] W. W. Daehnick, J. D. Childs, and Z. Vrcelj, Phys. Rev. C **21**, 2253 (1980).
[3] J. Bojowald, H. Machner, H. Nann, W. Oelert, M. Rogge, and P. Turek, Phys. Rev. C **38**, 1153 (1988).
[4] A. C. Betker, C. A. Gagliardi, D. R. Semon, R. E. Tribble, H. M. Xu, and A. F. Zaruba, Phys. Rev. C **48**, 2085 (1993).
[5] C. Bäumer *et al*., Phys. Rev. C **63**, 037601 (2001).
[6] A. Korff *et al*., Phys. Rev. C **70**, 067601 (2004).
[7] Qing-Biao Shen, Nucl. Sci. Eng. **141**, 78 (2002).
[8] B. Alder, S. Fernbach, and M. Rotenberg, *Methods in Computational Physics* (Academic Press, New York, 1996), Vol. 6.
[9] F. D. Becchetti, Jr. and G. W. Greenlees, Phys. Rev. **182**, 1190 (1969).
[10] R. L. Varner *et al*., Phys. Rep. **201**, 57 (1991).
[11] G. Igo, W. Lorenz, and U. Schmidt-Rohr, Phys. Rev. **124**, 832 (1961).
[12] T. Becker, U. Schmidt-Rohr, and E. Tielsch, Phys. Lett. **5**, 331 (1963).
[13] W. Fitz, R. Jahr, and R. Santo, Nucl. Phys. **A101**, 449 (1967).
[14] J. D. Childs, W. W. Daehnick, and M. J. Spisak, Phys. Rev. C **10**, 217 (1974).
[15] E. Newman, L. C. Becker, and B. M. Freedom, Nucl. Phys. **A100**, 225 (1967).
[16] F. Hinterberger, G. Mairle, U. Schmidt-Rohr, G. J. Wagner, and P. Turek, Nucl. Phys. **A111**, 265 (1968).
[17] K. Hatanaka, K. Imai, S. Kobayashi, T. Matsusue, M. Nakamura, K. Nisimura, T. Noro, H. Sakamoto, H. Shimizu, and J. Shirai, Nucl. Phys. **A340**, 93 (1980).
[18] G. Duhamel, L. Marcus, H. Langevin-Joliot, J. P. Didelez, P. Narboni, and C. Stephan, Nucl. Phys. **A174**, 485 (1971).
[19] Nguyen Van Sen *et al*., Phys. Lett. **B156**, 185 (1985).
[20] T. Ohnishi *et al*., Phys. Lett. **B438**, 27 (1998).
[21] H. Okamura *et al*., Phys. Rev. C **58**, 2180 (1998).
[22] Y. Satou *et al*., Phys. Lett. **B549**, 307 (2002).
[23] O. Aspelund, G. Hrehuss, A. Kiss, K. T. Knopfle, C. Mayer-Boricke, M. Rogge, U. Schwinn, Z. Seres, and P. Turek, Nucl. Phys. **A253**, 263 (1975).
[24] E. G. Auld, D. G. Crabb, J. G. McEwen, L. Bird, C. Whitehead, and E. Wood, Nucl. Phys. **A101**, 65 (1967).
[25] E. J. Stephenson, J. C. Collins, C. C. Foster, D. L. Friesel, W. W. Jacobs, W. P. Jones, M. D. Kaitchuck, P. Schwandt, and W. W. Daehnick, Phys. Rev. C **28**, 134 (1983).
[26] M. C. Radhakrishna, N. G. Puttaswamy, H. Nann, J. D. Brown, W. W. Jacobs, W. P. Jones, D. W. Miller, P. P. Singh, and E. J. Stephenson, Phys. Rev. C **37**, 66 (1988).
[27] V. R. Cupps, J. D. Brown, C. C. Foster, W. P. Jones, D. W. Miller, H. Nann, P. Schwandt, and E. J. Stephenson, Nucl. Phys. **A469**, 445 (1987).
[28] A. Kiss, O. Aspelund, G. Hrehuss, K. T. Knopfle, M. Rogge, U. Schwinn, Z. Seres, P. Turek, and C. Mayer-Boricke, Nucl. Phys. **A262**, 1 (1976).
[29] S. A. Hjorth and E. K. Lin, Nucl. Phys. **A116**, 1 (1968).

[30] S. I. Al-Quraishi, C. E. Brient, S. M. Grimes, T. N. Massey, J. Oldendick, and R. Wheeler, Phys. Rev. C **62**, 044616 (2000).
[31] R. Roche, N. Van Sen, G. Perrin, J. C. Gondrand, A. Fiore, and H. Muller, Nucl. Phys. **A220**, 381 (1974).
[32] G. Perrin, Nguyen Van Sen, J. Arvieux, R. Darves-Blanc, J. L. Durand, A. Fiore, J. C. Gondrand, F. Merchez, and C. Perrin, Nucl. Phys. **A282**, 221 (1976).
[33] A. Auce, R. F. Carlson, A. J. Cox, A. Ingemarsson, R. Johansson, P. U. Renberg, O. Sundberg, and G. Tibell, Phys. Rev. C **53**, 2919 (1996).
[34] T. Kawabata *et al*., Phys. Rev. C **70**, 034318 (2004).
[35] M. P. Bilaniuk, V. V. Tokarevskii, V. S. Bulkin, L. V. Dubar, O. F. Nemets, and L. I. Slyusarenko, J. Phys. G **7**, 1699 (1981).
[36] R. Jahr, K. D. Muller, W. Oswald, and H. Schmidt-Rohr, Zeitschrift fuer Physik **161**, 509 (1961).
[37] K. Bearpark, W. R. Graham, and G. Jones, Nucl. Phys. **73**, 206 (1965).
[38] J. R. Wu, C. C. Chang, and H. D. Holmgren, Phys. Rev. C **19**, 370 (1979).
[39] R. De Leo *et al*., Phys. Rev. C **53**, 2718 (1996).